

## Research Article

# Fault Detection Method of Medical Equipment Based on Multi-Index Electrical Performance Parameters

**Xiaoyu Chen** , **Haitao Guo**, **Zihong Wang** , **Feiba Chang**, **Xiaomei Ren**, **Chengqun Ma**, **Weiben Li**, **Miao Tian**, **Rui Yang**, **Xianju Yuan**, and **Shengting Zhou**

*Department of Medical Engineering, First Affiliated Hospital of Army Medical University, Shapingba, Chongqing 400039, China*

Correspondence should be addressed to Zihong Wang; wangzihong@tmmu.edu.cn

Received 10 July 2023; Revised 22 November 2023; Accepted 29 November 2023; Published 29 January 2024

Academic Editor: Giovanni Diraco

Copyright © 2024 Xiaoyu Chen et al. This is an open access article distributed under the Creative Commons Attribution License, which permits unrestricted use, distribution, and reproduction in any medium, provided the original work is properly cited.

There is a lack of study on fault detection methods of medical equipment at home and abroad. The main reason is that the research of fault features is diverse and not systematic. This paper aims to propose a fault recognition method for medical equipment combining the electrical performance parameter features with fault events. First, it treats the equipment as a whole system, setting up the analysis model. Then, we are going to analyze the signal for indicator. This paper chooses the multi-index electrical performance parameters (MEPP) method for the fault identification an indicator. It is proved that the electrical performance signal can evaluate the status of equipment. Thus, it can also be used to recognize the fault or other working statuses. Then, the features of current, voltage, and power are studied exhaustively using a mathematical model. After that, the weight of each parameter feature in any specific event will be determined according to the influence of each parameter feature on fault events. At that time, the recognition method basically realizes the correlation between multi-index features and fault events through weight. Next, the above method needs to be verified in the experiment. This paper chooses six monitors for setting the rules of normal status. The normal status is the baseline for fault identification. Then, feature intervals of other faults are established around this reference. Finally, each feature interval will be constantly adjusted to meet the preset recognition rate and updated to the rules in the subsequent measurement. In this paper, 10 monitors are selected as samples to update a set of basic judgment rules based on MEPP, and by adjusting the overlapping interval, the fault recognition rate reaches more than 90% in this study. To sum up, this paper uses the MEPP method to find out the relationship of features of current, voltage, and power with fault events. It will become a new direction for fault recognition studies on electrical medical equipment and other device.

## 1. Introduction

The current fault diagnosis technology usually applies the equipment status of physical features from events or historical status knowledge to evaluate the equipment status through certain analysis methods (such as analysis of signal processing) [1, 2]. It is actually a direct evolution from the artificial fault diagnosis method. However, there are obvious differences of fault recognition between the artificial and the machine, especially in the means of fault feature extraction and analysis. The current fault diagnosis technology in academic research is not effective. The main reason is that it is not a closed loop because the study of the fault characteristic principle is not enough, and the traditional preparation conditions for measurement are high. For example, Song et al. [3]

proposed a kind of intelligent identification method based on deep learning fault diagnosis technology. Although it requires the assistance of mathematical models a little, but it needs long-term knowledge, high requirements for engineers, time of constructure and verification methods. The research of fuzzy fault detection for industrial equipment has been able to meet the requirements. For the accurate fault identification of electrical equipment, it needs to be further deepened in all aspects of design [3]. Another example is Liu et al.'s [4] research that the rule of fault diagnosis method is based on general expert knowledge, which combines expert experience for fault diagnosis. It expresses the previously input experience knowledge through one or several ways and translates it into the machine according to the artificial reasoning technology and diagnosis strategy for machine fault recognition [4].

For medical equipment, Li et al. [5] proposed the fuzzy decision method and association mining method by using the data OFWSC algorithm. It is a kind of improved method for event association [5]. The above methods are similar. It is currently a mainstream method of fault recognition using the association of expert knowledge. Although in recent years, the development of artificial intelligence technology has promoted the development of fault diagnosis technology from traditional technology to intelligent technology, and artificial intelligence has gradually replaced artificial detection, the theoretical research of fault identification is still weak, and the theoretical research needs to establish a certain mathematical model [6–9].

Another research topic is to establish the mathematical model of the medical equipment through the electrical, acoustooptic, and other physical feature parameters of the medical equipment. Then, some researches discuss the specific features of the medical equipment which cannot work normally in theory. Zhang et al. [10] chose to research the status of the power supply circuit module, and use feature fusion to extract morphological features and temporal features. It still combines applying fault recognition with correlated events. However, this research has the establishment of mathematical models to achieve feature extraction. It needs to be very familiar with the structure of the specific equipment if it is necessary to apply it by the research. This research also shows the professional degree of power supply circuit modules to analyze accurately [10]. This team has done a lot of research on the signal output of devices, reflecting the current research upsurge upon fault identification through components [11–13]. However, component detection is of great help to analyze theoretically and theoretical model building. However, there are few related researches, and the implementation is relatively complex, which requires medical researchers being professional in electrical theory knowledge and structural modules of equipment.

In actuality, event correlation and mathematical modeling complement each other's shortcomings during the course of fault recognition research, representing theoretical exploration and practical experience, respectively. To address the aforementioned issues, further improvements in fault recognition and judgment methods are required. In the past, the study of medical equipment fault events had been correlated with the electrical performance by anyone. In this paper, a new fault recognition method combining electrical characteristics with fault events is proposed. Initially, the paper scrutinizes the characteristics of the output signal of medical electrical equipment, taking the monitor as an example, and extracts the features of its output signal. Additionally, a fault detection method based on multiple parameters is proposed, utilizing three types of electrical signals commonly generated by equipment: current, voltage, and power, for acquisition and processing. These signals embody the electrical performance features of the equipment during shutdown and standby states. Through the decomposition of a signal mathematical model, the theoretical expression formulas for three types of electrical performance parameters are derived. Subsequently, the paper utilizes different signal features to represent distinct equipment states and verifies this through

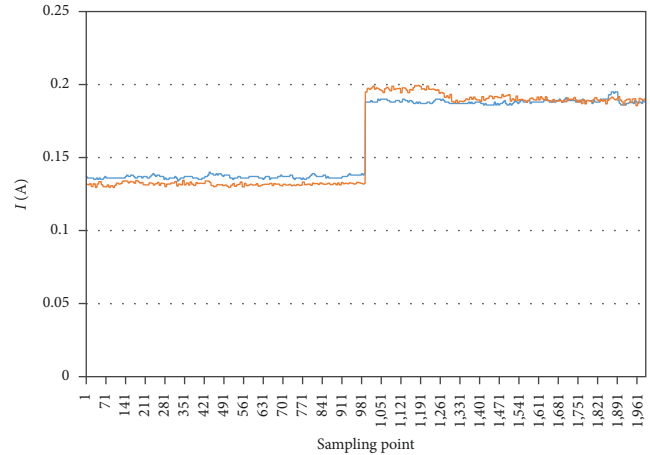


FIGURE 1: Monitors cable fault and normal.

actual measurements of normal and faulty states on other identical model equipment. Ultimately, the relationship between faults and features is investigated.

## 2. Theoretical Basis Research

**2.1. Preliminary Basic Experiment.** Fault recognition research can combine the electrical performance parameters with the fault features. As the current of some medical equipment is an example, its signal is shown in Figure 1.

The data of the electrical performance parameters is almost stable. However, the stability will be determined by the robustness of the outer sensors, which leads to the convergence rule of the different status from multiple equipment of the same brand and specification.

We're guessing that the output signal of current is a constant when some medical equipment is in the steady status. To prove it, this paper designs an experiment. Taking the monitors as an example, they list some of the status of normal equipment to measure the current. Then, we list a kind of faulty equipment to check whether the current signal performs as the normal one. It is shown in Figure 2.

Figure 2(a) shows the current signal of a certain type of monitor in different statuses. The horizontal axis means sampling points, and it represents the frequency of 3 Hz (every three points equal to 1 s). The vertical axis is the current A. Each stage of the signal in Figure 2(a) represents the running status as follows: ① represents power off, ② represents power-on moment, ③ represents standby, ④ represents noninvasive blood pressure testing; ⑤ represents a fault: the display is powered off, ⑥ represents that the equipment restarted under this fault, ⑦ represents that the display still power off, ⑧ represents another fault: the main control board failed. Figure 2(b) shows the current value under the on/off status of the monitor, with the main control board faulty and the normal one on the same model (high level is power on, low level is power off). From Figures 2(a) and 2(b), it can be seen that the electrical performance features of the equipment will indicate the statuses of the equipment. The change of status will also lead to the change of electrical signal. The mean value can be used as the

TABLE 1: Current mean value of a certain type of monitor under various faults.

| Value name               | Status name |            |                 |                      |                  |                |
|--------------------------|-------------|------------|-----------------|----------------------|------------------|----------------|
|                          | Normal      | ECG fault  | Mainboard fault | Display screen fault | Main cable fault | Air pump fault |
| Average shutdown current | 0.140 A     | 0.137 A    | 0.051 A         | 0.122 A              | 0.122 A          | 0.141 A        |
| Average stand by current | 0.205 A     | 0.188 A    | 0.139 A         | 0.188 A              | /                | 0.196 A        |
| Threshold range          | (−6, 6 mA)  | (−5, 5 mA) | (−5, 5 mA)      | (−5, 5 mA)           | (−5, 5 mA)       | (−5, 5 mA)     |

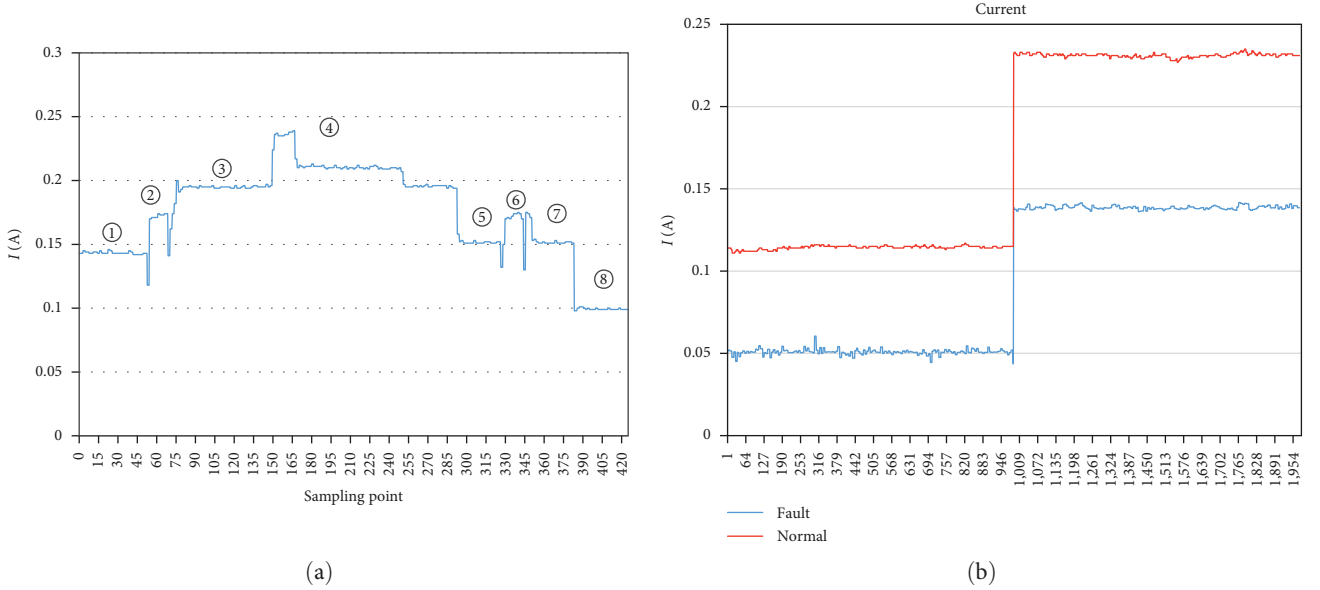


FIGURE 2: Current of monitor: (a) monitor under different working conditions; (b) current of normal and faulty equipment.

feature parameter because of the steady status of the electrical signal output.

After calculating and analyzing a large number of data collected from preliminary experiments, we have obtained the fault performance of the monitor known is obtained and summarized it with features of current in Table 1.

Among them, each status has a fluctuation range. According to the current measured data, the fluctuation range is less than 2%. The accuracy of judging some faults can be more than 90%, such as the main cable fault and the mainboard fault. However, this method is not convinced to judge the other faults like air pump faults. The computer will not calculate the point falling in the threshold range of standby or shutdown only, but also in “standby + shutdown” meanwhile. It proves that the current signal of equipment working in each stable status is almost a straight line.

**2.2. Theoretical Model.** It can be seen from the basic circuit calculation formula  $U = I^2R$  that the smaller the resistance of the equipment at rated power, the greater the current is. From Figures 1 and 2, this kind of medical equipment can be simulated as a linear system because the signal can be changed by the status. Besides, it can be seen from Figure 2(a) that the feature of a signal can be related to the changes of status. It conforms to the law of linear systems and the basic electrical formula [14].

According to the medical equipment characteristics, the total signal output of medical equipment can be simulated

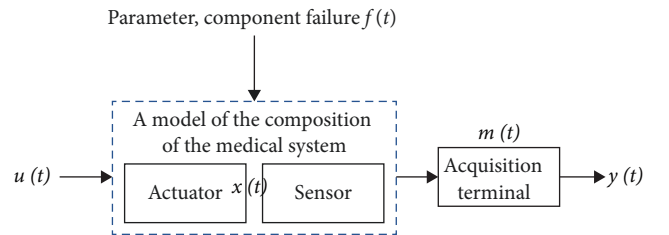


FIGURE 3: Electrical signal model of medical equipment.

into two categories—the sum of output from the actuator system and the sensor system that these two systems generate time-related signals, respectively. When the fault occurs, the faulty signal is superimposed into the total signal output by the equipment according to linear system characteristics [15]. The medical equipment can be simulated in Figure 3.

However, the output signal of the device is difficult to obtain directly. It needs to be collected by external sensor measurement. At this time, the external sensor, as an independent system, will also cause the new signal component, which will be superimposed into the entire output of the system to form a kind of output signal named observation signal output. The observation output signal can be expressed as follows:

$$y(t) = Ax(t) + Bu(t) + R_1f(t) + Cm(t), \quad (1)$$

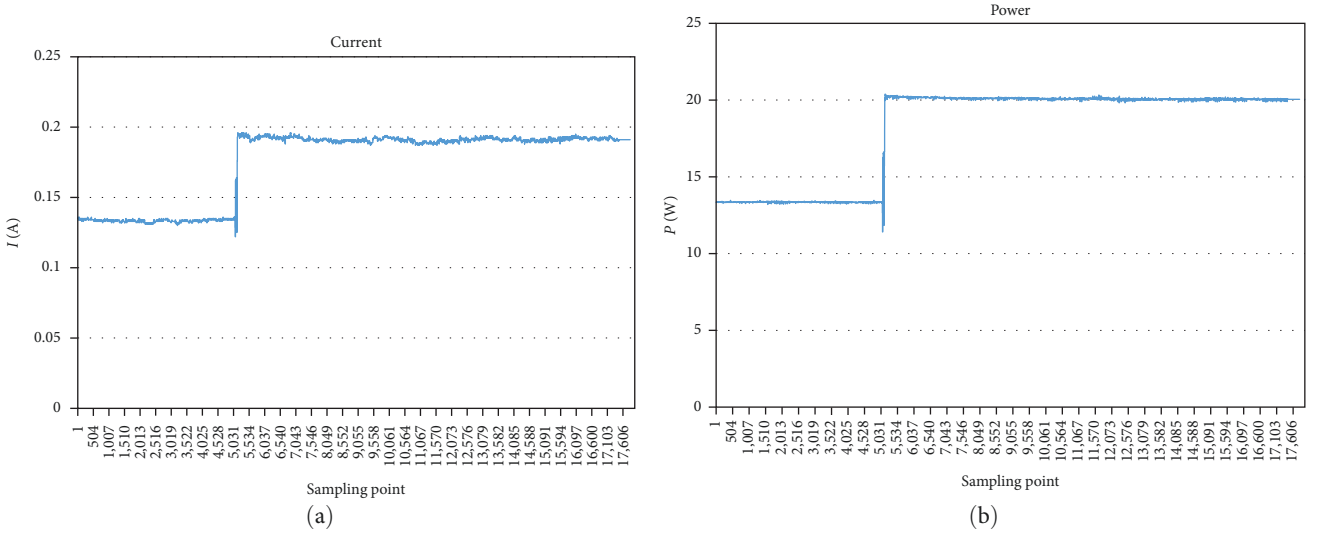


FIGURE 4: Current and power under on and off power status.

where  $\mathbf{x}(t)$  is the status vector,  $\mathbf{u}(t)$  is the control vector,  $\mathbf{x}(t) \in R^n$ ,  $\mathbf{u}(t) \in R^p$ , respectively. These two are the system operation vector and controller output signal vector under the normal statuses of the equipment.  $\mathbf{y}(t)$  is the observation output signal vector.  $\mathbf{m}(t)$  is the signal vector added by the external sensor and is the signal output added by the external acquisition sensor itself.  $\mathbf{f}(t)$  is the vector of the abnormal running status of the equipment.  $\mathbf{f}(t) \in R^g$ . Each element  $f_i(t)$  ( $i=1, 2, 3, \dots, n$ ) means the specific kinds of fault. It is also a function of time that we need to solve in fault recognition research.  $\mathbf{ABC}$  is the constant value matrix of the corresponding dimension.  $\mathbf{R}_1$  is the fault coefficient matrix, and the dimension of the matrix is determined by the number of detectable statuses.

**2.3. Current and Power Signal Analysis.** Among various representable signals of equipment, current and voltage can be easily collected and represented, while power can be obtained by current and voltage as a kind of new indicator through processing. Take the current as an example because the current is approximately a fixed value during steady status operation (the fluctuation comes from the robustness of the acquisition sensor itself). This paper mainly studies the features of electrical signals when a single fault occurs, so suppose that when the monitor is in a certain fault, the current is when it is turned off, and the current is when the monitor is on standby, and they are taken into Equation (1) to get the following:

$$\begin{cases} i_1(t) = a_1x_1(t) + b_1u_1(t) + r_1f_1(t) + c_1m_1(t) \\ i_2(t) = a_2x_2(t) + a_2u_2(t) + r_2f_2(t) + c_2m_2(t) \end{cases} \quad (2)$$

According to the data obtained from the experiment, the equipment working in steady status can output constant signals only because it is or periodic signals but mutually canceling each other. However, the consistency of a large number of experimental results shows that it is almost

impossible to make coincidentally the superimposed signals to cancel each other for every time. Therefore, here, it considers that the equipment working in steady status can output constant signals, and it contains the margin of error due to robustness. Equation (2) can be transformed as follows:

$$\begin{cases} i_1(t) = a'_1 + b'_1 + c_1m_1(t) \\ i_2(t) = a'_2 + b'_2 + c_2m_2(t) \end{cases} \Rightarrow \mathbf{i}^T_{\text{Nor}}(t) = \begin{vmatrix} i_1(t) \\ i_2(t) \end{vmatrix}. \quad (3)$$

The external sensor output signal is still considered to when  $m(t)$  remains unchanged.

However, the fault analysis also has much limitation, especially using one of the parameters. It is impossible to accurately locate the fault features by only one indicator. Some relative experiments show that it affects the normal working electrical equipment a little or not when some accessory module fails. Accessory modules like the ECG connection cable on a monitor, the flow sensor of the ventilator or the electrode plate of the defibrillator. This paper introduces other parameters—voltage and power. At the same time, the experiment shows that the current and power of the device also maintain a stable signal output whenever the device is on or off power, as shown in Figure 4.

The current and power signals can be represented as follows:

$$\begin{cases} \mathbf{i}(n) = \mathbf{i}_0 + \mathbf{cm}(n) + \mathbf{rf}_i(n) \\ \mathbf{p}(n) = \mathbf{p}_0 + \mathbf{iq}(n) + \mathbf{vf}_p(n) \end{cases} \quad (4)$$

The sampled data points are discrete distribution, so there switched the variable from time to “ $n$ ” which means discrete distribution points representing the corresponding relationship of each single sampling point. So  $\mathbf{i}(n)$ ,  $\mathbf{p}(n)$ , respectively, represents the  $n \times 2$  times matrix of current sampling value and power sampling value under the status of power off and standby from the observation of external

sensors. “ $n$ ” represents the number of fault types, and “2” represents the two kinds of status—power off and standby.  $\mathbf{m}(n)$  represents the matrix of current sampling value when the external sensor circuit measures the status from power off and standby.  $\mathbf{q}(n)$  represents the matrix of power sampling value when the external sensor circuit measures the status from power off and standby.  $\mathbf{f}_i(n), \mathbf{f}_p(n)$  is the matrix of current sampling value and the power sampling value at the running status.  $\mathbf{i}, \mathbf{c}, \mathbf{r}, \mathbf{p}, \mathbf{e}, \mathbf{v} \in \mathbf{R}^{n \times 2}$  [16].

**2.4. Feature Extraction and Voltage Signal Analysis.** Based on the characteristics of Figure 2, this paper introducing the method of residual measurement. The reason is below:

- (1) It should be obvious how the features combine with the status events.
- (2) Features can be changed by the change of status events and it should be one-to-one correspondence.
- (3) The features reflect the characteristics of the signal. It can be seen from Figures 2 and 3 that the current and power have the characteristics of numerical differences under different status events.

So, the fault features in Equation (6) can be transformed based on the residual measurement method as follows:

$$\begin{cases} \beta = \mathbf{r}\mathbf{f}_i(n) + \mathbf{j} \\ \chi = \mathbf{v}\mathbf{f}_p(n) + \mathbf{k} \end{cases}, \quad (5)$$

$$\left( \mathbf{j} \in \cup_{i=0}^n (\mathbf{i}_{fault}(n) - \bar{\mathbf{i}}), \mathbf{k} \in \cup_{i=0}^n (\mathbf{p}_{fault}(n) - \bar{\mathbf{p}}) \right). \quad (6)$$

As can be seen from Equation (7), the fault features  $\beta, \chi$  can be obtained by the fault signal of current and power subtracted from normal signals. That is the point of residual measurement.  $\mathbf{j}, \mathbf{k}$  represents as the margin of error. To the features, it means feature range. Finally, the normal one’s current is used as the reference value to compare with the actual measured value, and the features  $\beta, \chi$  of the fault value are used as the difference. The fault and normal current and power can be expressed as the following relationship by the characteristic value:

$$\begin{cases} \mathbf{i}_{fault}(n) = \mathbf{i}_{normal}(n) + \beta \\ \mathbf{p}_{fault}(n) = \mathbf{p}_{normal}(n) + \chi \end{cases}. \quad (7)$$

When finds a new fault and define its range, it is only to use the measured signal to subtract the value of the normal according to the sampling frequency. If it identifies the status type, it only needs to compare the signal existing in which the status feature range of the equipment is measured. In order to reduce the calculation complexity, this paper adopts the method of window translation for sampling, and the width of the sampling window is 10 s. At this point, the feature extraction of this kind of signal is complete. As for the voltage signal, the voltage fluctuates periodically in theory. Through measurement, it is found that it accords with the theoretical

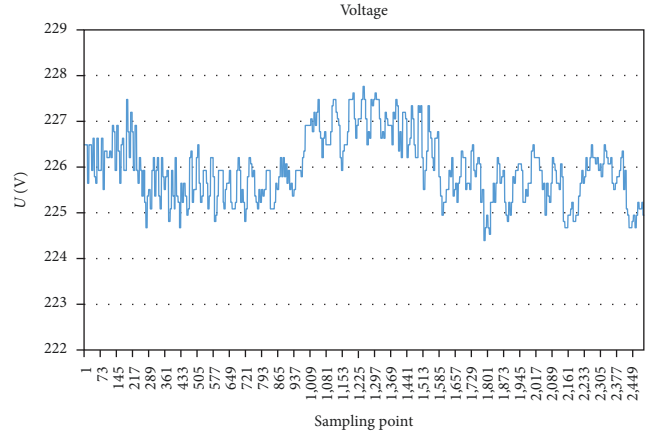


FIGURE 5: The voltage under off power and standby.

signal characteristics by measurement. Because of the interference caused by the actual measured environmental factors, the signal does not fully conform to the sine and cosine functions. It is shown in Figure 5.

From Figure 5, we can see that there is no significant change in signal characteristics between the power off and standby. We can conclude that there are two basic principles for the extraction of characteristic signals as follows:

- (1) The error range of a single status sampling signal shall not exceed 5% within one cycle.
- (2) Signal changes obviously with the change of status.

Although it is impossible to extract voltage features effectively through only the current means, the more conditions, the higher accuracy when the fault recognition method is the MEPP. Besides, this paper will mention how to use three kinds of parameters to avoid the interference of invalid features. The output of voltage can still be expressed as a distributed formula about “ $n$ ”. It can be expressed as below:

$$\mathbf{v}(n) = \mathbf{d}\mathbf{v}_0(n) + \mathbf{e}\mathbf{u}(n) + \mathbf{o}\mathbf{s}(n) + \mathbf{s}\mathbf{f}_v(n), \quad (8)$$

where  $\mathbf{x}(n)$  is the status voltage sampling value matrix when the equipment is off power and standby.  $\mathbf{u}(n)$  represents the control signal voltage sampling value matrix when the equipment is off power and standby.  $\mathbf{s}(n)$  represents the external circuit sensor voltage sampling value matrix when the equipment is off power and standby.  $\mathbf{f}_v(n)$  represents the voltage sampling value matrix of the abnormal running status signal.  $\mathbf{d}, \mathbf{e}, \mathbf{o}, \mathbf{s} \in \mathbf{R}^{n \times 2}$  represents all belong to  $n \times 2$  times matrix. The characteristic value of voltage is as follows:

$$\begin{cases} \mathbf{v}_{fault}(t) = \mathbf{v}_{normal} + \delta \\ \delta = \mathbf{s}\mathbf{f}_v(n) + \mathbf{l} \end{cases} (\mathbf{l} \in \cup_{i=0}^n (\mathbf{v}(n) - \bar{\mathbf{v}})). \quad (9)$$

From the above, the three kinds of electrical parameters of the equipment have realized feature extraction. The essence of MEPP is aimed to use more features and conditions for helping fault recognition. Besides, some status

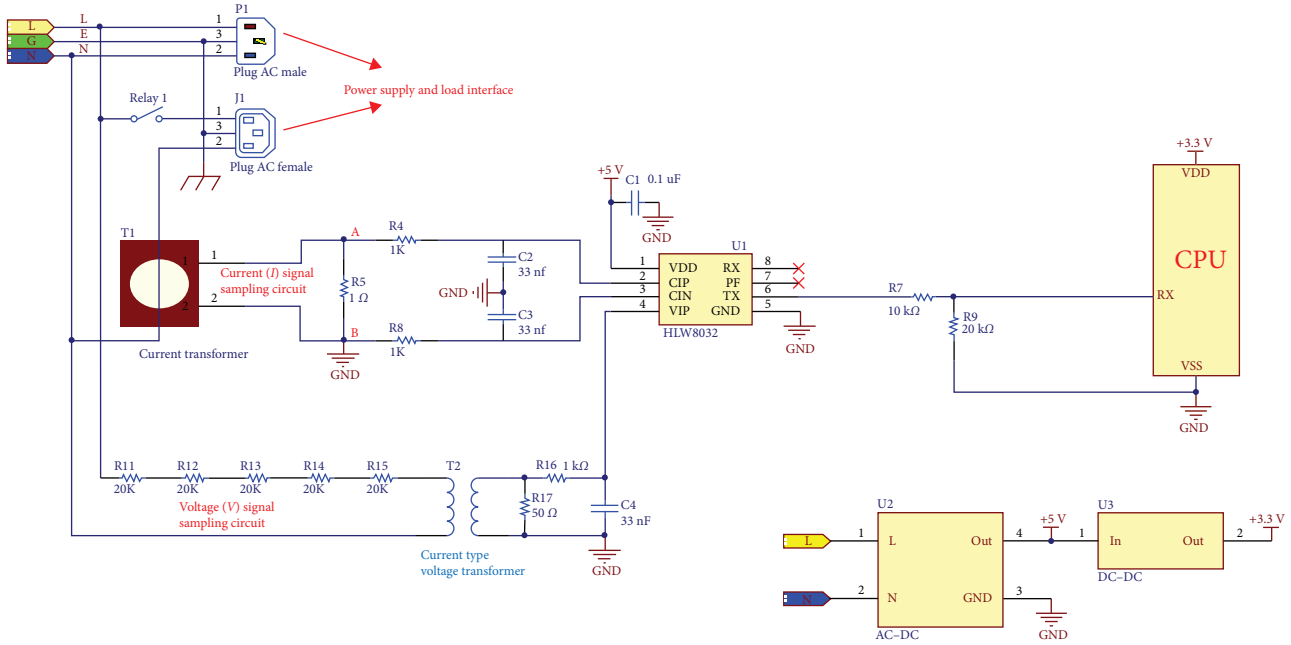


FIGURE 6: Schematic diagram of the measurement module.

events can be easily recognized by voltage at later research found. Next, this paper then uses the judgment logic–concise correlation knowledge to classify the features to achieve the goal of fault recognition.

### 3. Materials and Methods

**3.1. Hardware Facility.** The signal from equipment output could not be obtained directly. It should be measured by an outer sensor. In this paper, HLW8032, as a single-phase metering chip, is used for the collection and calculation for power. Three kinds of parameters are obtained from the sensor circuit as follows:

$$\begin{aligned} U_{\text{rms}} &= \frac{\eta}{\kappa} \times \frac{R_1}{R_2 \times 1,000} \\ I_{\text{rms}} &= \frac{\theta}{\sigma} \times \frac{R_3}{R_4 \times 1,000} \\ P &= U_{\text{rms}} \times I_{\text{rms}} \end{aligned} \quad (10)$$

For the external sensor, the measured values of the three parameters are not the original. They are converted into effective values through the sensor circuit, which will affect the components and structure in the circuit. So,  $U_{\text{rms}}$ ,  $I_{\text{rms}}$  from the above formula represents the effective value of voltage and current,  $\eta$ ,  $\theta$  represents the voltage and current parameter register.  $\kappa$ ,  $\sigma$  represents the voltage and current register.  $R_1$ ,  $R_2$ ,  $R_3$ ,  $R_4$  represents the resistance value in series and parallel in the sensor circuit [17].

The measured values of each parameter in Equation (1) mainly depend on the circuit design of the external acquisition terminal. The acquisition terminal is not limited to the design adopted in this paper, and there is no need to conform to the standards of the acquisition terminal for the same.

Subsequent research can be designed by any group of design parameters according to needs. The design of this paper is shown in Figure 6.

In this paper, the hardware deployment adopts the interventional power replacement method. The specific implementation steps are as follows: replace the equipment's own power supply with a sensor. The sensor replaces the medical equipment's to provide AC 220V/50Hz to the equipment. At the same time, the sensor detects the working electrical parameters, voltage current, and power of the equipment in real time. The collected electrical performance parameters are sampled by the MCU of the sensor and are sent data wirelessly to the server of the fault identification system. The server stores and analyzes the data to identify and mark the abnormal data through the set threshold value with the fault identification method. Finally, the data result is displayed on the PC through the WEB. Based on the hardware set up in Figure 5, the actual measurement of the equipment is carried out in this paper. The connection diagram is shown in Figure 7.

**3.2. The Establishment Method of Fault Rule Database.** Based on the existing knowledge, this paper establishes the association rules of fault events and electrical features and classifies fault features as a system. The system assumes that electrical performance parameters are the items, and  $\mathbf{T}_n$  as the fault electrical features in a moment.  $\mathbf{T}_n$  can be expressed as follows by Equations (7) and (9):

$$\mathbf{T}_l = \{\mathbf{i}_{nl}, \mathbf{v}_{nl}, \mathbf{p}_{nl}\} = \begin{bmatrix} i_{1l} & v_{1l} & p_{1l} \\ i_{2l} & v_{2l} & p_{2l} \end{bmatrix}, \quad (11)$$

where  $\mathbf{i}_{nl}$ ,  $\mathbf{v}_{nl}$ ,  $\mathbf{p}_{nl}$  represents the sampling value matrix of current, voltage and power.  $n$  represents the kinds of working status. This paper chooses two kinds of working statuses—power off and standby.  $l$  represents the operation status

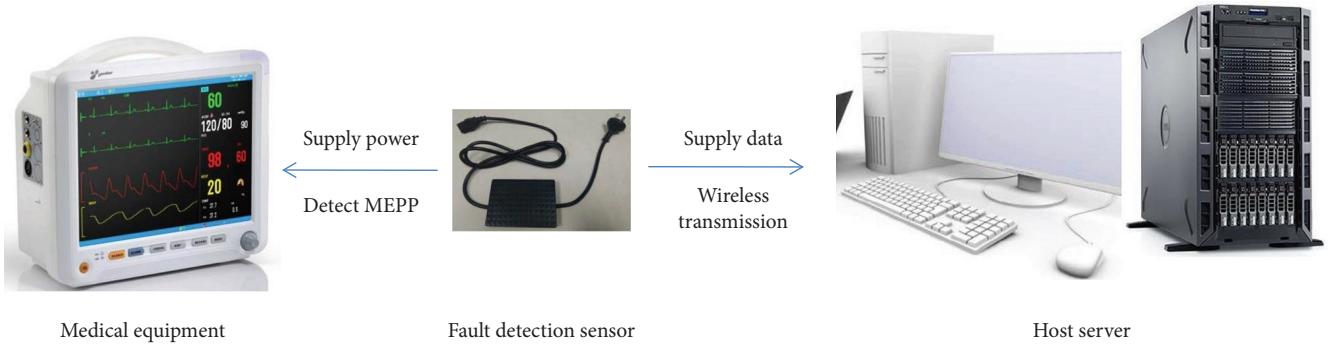


FIGURE 7: Schematic of detection system working.

TABLE 2: The list of known faults.

| Status               | Fault performance  | Status recognition | Characters value            |
|----------------------|--|--------------------|-----------------------------|
| Normal               | \  | A                  | $\beta_0, \chi_0, \delta_0$ |
| ECG fault            | ECG waveform is irregular or measured without waveform                     | $B_1$              | $\beta_1, \chi_1, \delta_1$ |
| Mainboard fault      | The main control system fails to turn on or proceed other control function | $B_2$              | $\beta_2, \chi_2, \delta_2$ |
| Display screen fault | The screen is none when switch on, and no operation is displayed           | $B_3$              | $\beta_3, \chi_3, \delta_3$ |
| Main cable fault     | Clicking keys fault. It is unable to turn on and off or other operation    | $B_4$              | $\beta_4, \chi_4, \delta_4$ |
| Air pump fault       | It fails to inflate when noninvasive blood pressure measures               | $B_5$              | $\beta_5, \chi_5, \delta_5$ |

containing the normal and various fault types. All features are associated with the fault events to form a complete database, which is expressed as  $T = \{T_0, T_1, T_2, \dots, T_l\}$ .  $T_0$  represents the system in normal status which also means the initial status or reference status. There are “ $l$ ” kinds of fault in total and  $l \in N$ .

This paper chooses existing knowledge as the basis for system training, which can not only accurately diagnose equipment fault events but also sort out some repair suggestions and troubleshooting experience. At this time, according to the previous experience from the Medical Engineering Department, this paper lists known faults. Besides, this paper chooses a specific equipment, for example—monitor, a kind of first aid equipment. The known faults are shown in Table 2.

Fault features and status events should be related [18]. It requires a set of logic methods to connect these two elements into a system, which should be a kind of closed loop as well. First of all, the fault events and the fault features are corresponding to each other in theory. The law of fault recognition is to recognize which characteristic interval belongs to from the measurement of electrical parameters value by observing the probability distribution of some particular status named the probability of distribution. Based on this principle, the fault events should exist in the causal relationship. So this relationship can be represented in Figure 8.

Figure 8 shows the basic rules and logic of building the fault feature database. This database should have the following characteristics:

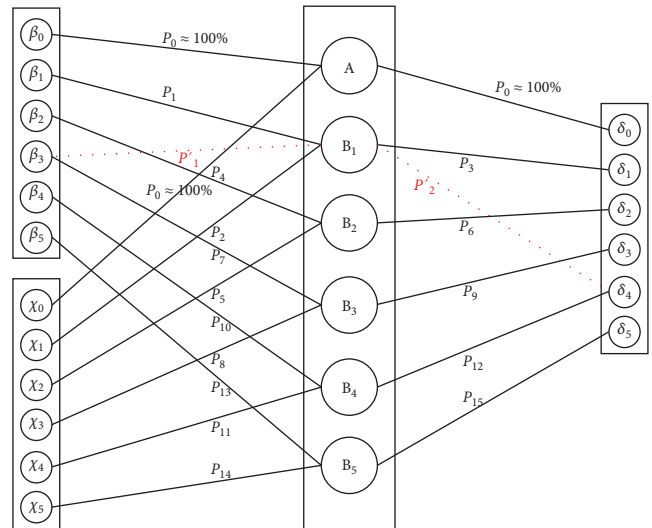


FIGURE 8: The causal relationship between the fault events and features.

- (1) The corresponding fault events and features are probabilistic, and there is a specific probability distribution.
- (2) Specific distribution probabilities can be calculated by actual measurements.
- (3) The whole process of fault identification should be closed-loop and updatable.

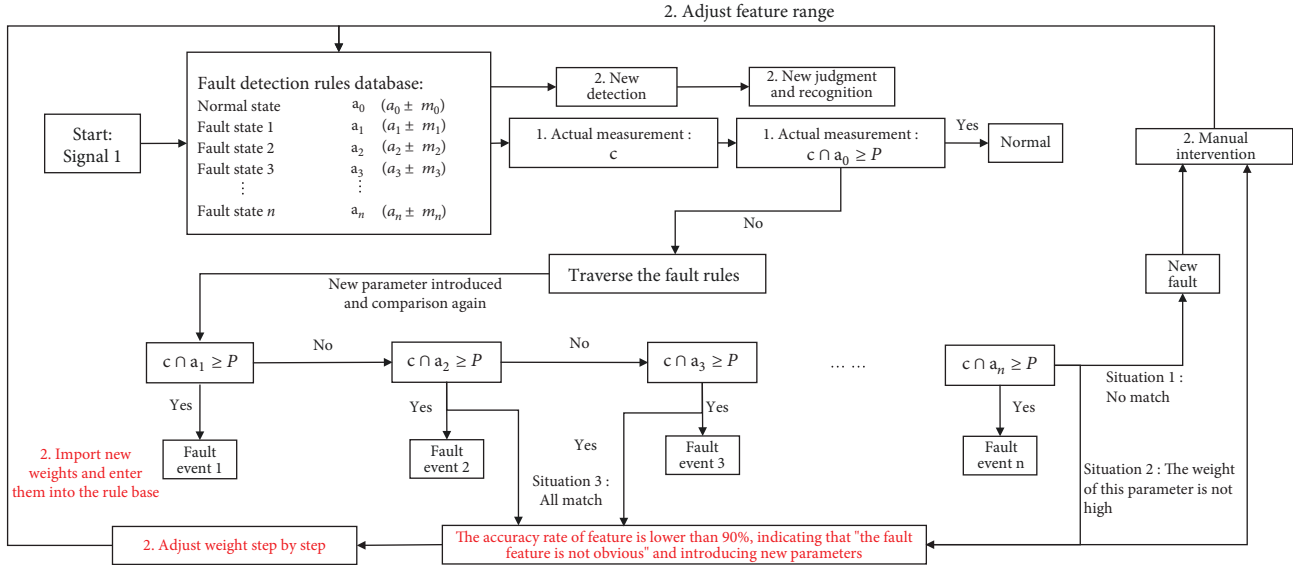


FIGURE 9: The logical judgment method of each electrical performance parameter.

TABLE 3: Rules of weight setting.

| $P$ (%)        | $\theta$ | $P$ (%)        | $\theta$ | $P$ (%)        | $\theta$ | $P$ (%)        | $\theta$ | $P$ (%)        | $\theta$ |
|----------------|----------|----------------|----------|----------------|----------|----------------|----------|----------------|----------|
| $\geq 90$      | 9        | $90 > \geq 80$ | 8        | $80 > \geq 70$ | 7        | $70 > \geq 60$ | 6        | $60 > \geq 50$ | 5        |
| $50 > \geq 40$ | 4        | $40 > \geq 30$ | 3        | $30 > \geq 20$ | 2        | $20 > \geq 10$ | 1        | $10 >$         | 0        |

(4) It should have a set of rules that, in theory and work.

From Figure 8, we can know that  $P_0$  represents the distribution probability of normal status.  $P_1 - P_{15}$  represents the distribution probability of the fault features collected from each status event. The logic of the whole system is that events and features are combined together through probability.

Theoretically, each status must be only associated with a specific group of features. The event-related fault recognition method only needs to combine fault features with fault events. It can be seen that there are no other elements in the whole causal event except distribution probability and fault event. Let's assume that the normal status signal feature  $P_0$  needs to cover the whole sampling point of the electrical performance parameters under normal equipment conditions as far as possible because the normal status is a kind of largest number statuses in nature. This paper will treat the normal status as the initial status of the database and the status judgment of all statuses.

Not every feature of every status event is completely independent from the corresponding feature of other status events. Among the actual measurements, it is found that the distribution probability range of the same kind of feature is highly coincident under different fault events. Taking fault event  $B_1$  as an example, it indicates that the feature  $\beta_1, \beta_3$  and  $\delta_1, \delta_3$  may be highly coincident. It leads that the distribution probability of  $\beta_3, \delta_4$  may produce  $P'_1$  and  $P'_2$ , which may cause interference during  $B_1$  fault recognition. However, the most ideal effect is that the fault event  $B_1$  should only

corresponds to  $\beta_1, \chi_1, \delta_1$ . In order to solve this problem, the method of processing data in this paper adopts that three kinds of parameters are ranked according to their importance, and there will make a comparison for judgments as order. Each parameter feature is compared to the fault rule base by traversing. Finally, it finds a method in that even if the feature distributions of certain electrical performance parameters coincide, each of the two statuses can be distinguished. The logical judgment method of each electrical performance parameter is shown in Figure 9.

**3.3. The Fault Judgment of Weighted Method Based on Events Association Rules.** When the fault rules work, there will generate a rate which is the distribution probability of the current, the voltage, and the power falling points under the characteristic range, expressed as  $P_1, P_2, P_3$ , respectively. According to Equations (7) and (9), three kinds of electrical performance parameters can be obtained, and each characteristic value can be calculated when the equipment suffers from the above faults. Since the physical meaning of the three parameters is independent, the joint judgment process will calculate introducing the weighting to unify a total status of recognition rate. This paper uses the AHP-like method to determine the weight, which is a kind of research method for calculating the weight qualitatively and quantitatively. It compares the number size of each two elements while the larger the number, the more important it will be, and finally gains the weight of each element. Therefore, the recognition rate after adding the weight can be expressed as follows:





FIGURE 10: Current comparison of six normal monitors.

$$\mathbf{P} = \frac{\theta_1 \times \mathbf{P}_1 + \theta_2 \times \mathbf{P}_2 + \theta_3 \times \mathbf{P}_3}{\theta_1 + \theta_2 + \theta_3}, \quad (12)$$

where  $\mathbf{P}_1$ ,  $\mathbf{P}_2$ ,  $\mathbf{P}_3$  represents the fault recognition rate of current, power and, voltage while  $\theta_1$ ,  $\theta_2$ ,  $\theta_3$  represents the weight of the three features. Since there are two working statuses, the above six parameters are all  $1 \times 2$  order matrices. The weight can be assigned, according to the following rules, as shown in Table 3.

The adjustment rules of  $\theta$  can be infinitely optimized in accordance with the needs of better and better accuracy. It can be seen from Table 3 that the step size of  $P$  is 10% and the step size of  $\theta$  is 1. We can make more accuracy that the step size of  $P$  change to 5%, 2%, or less, and the step size of  $\theta$  change to 0.5, 0.2, or less correspondingly.

The function of weight aims to adjust the value of the total recognition rate flexibly. Equation (12) gains  $\mathbf{P}$ . The represents the total probability from the status event of power off and standby. It determines the final probability of the status from actual measurement. The whole system of fault recognition is around this indication. For more accuracy, this paper defines that the total recognition probability should be  $\geq 90\%$  to judge one specific status event. To achieve

this goal, this paper will adjust  $\theta_1$ ,  $\theta_2$ ,  $\theta_3$  while the actual measurement.

## 4. Experimental Verification

**4.1. Measurement and Input for Reference Base Rule.** In order to verify the feasibility of the above system, we then carry out actual measurements of some equipment and build a database. Taking the monitor as an example, six normal monitors of the same model are selected for measurement. First, all electrical features of six normal monitors in the on and off statuses are collected and analyzed to initially establish the benchmark features of the normal status of the monitors in the fault database. The current comparison of the six normal monitors is shown in Figure 10.

Calculating the mean value for the benchmark value of the current and the fluctuation range interval of the feature range in the above graph gives the benchmark value and the feature interval. The data are shown in Table 4.

According to the current data collected from the six normal monitors, it can be found that the benchmark values of each monitor in the on and off statuses are basically similar, which is in line with the findings of the previous theoretical study. Based on the data in Table 3, the benchmark value in

TABLE 4: Current features of the six normal monitors.

| Status | No. 1             |              | No. 2             |              | No. 3             |              |
|--------|-------------------|--------------|-------------------|--------------|-------------------|--------------|
|        | $i_{normal}$ (mA) | $\beta$ (mA) | $i_{normal}$ (mA) | $\beta$ (mA) | $i_{normal}$ (mA) | $\beta$ (mA) |
| Off    | 145               | (-3,3)       | 153               | (-2,3)       | 150               | (-4,3)       |
| On     | 208               | (-5,7)       | 202               | (-4,4)       | 201               | (-3,6)       |
| Status | No. 4             |              | No. 5             |              | No. 6             |              |
|        | $i_{normal}$ (mA) | $\beta$ (mA) | $i_{normal}$ (mA) | $\beta$ (mA) | $i_{normal}$ (mA) | $\beta$ (mA) |
| Off    | 149               | (-5,3)       | 153               | (-5,6)       | 153               | (-6,7)       |
| On     | 212               | (-4,6)       | 204               | (-3,2)       | 203               | (-4,5)       |

TABLE 5: Features of the three electrical properties of the six normal monitors.

| Status and features   | Current (mA) | Voltage (V)  | Power (W)    |
|-----------------------|--------------|--------------|--------------|
| Off                   |              |              |              |
| $i_{normal}$          | 152          | 226.17       | 17.50        |
| $\beta, \chi, \delta$ | (-7,6)       | (-2.61,1.74) | (-1.5,2.1)   |
| On                    |              |              |              |
| $i_{normal}$          | 206          | 226.91       | 23.84        |
| $\beta, \chi, \delta$ | (-6,6)       | (-1.83,1.91) | (-1.18,2.70) |

the off status can be set to 152 mA, and the benchmark value in the on status can be set to 206 mA. According to Figure 8, when the filter criteria are set as the recognition rate is greater than 90%, the data of six monitors are basically covered in this recognition interval, and to achieve the narrowest feature interval, it can be set to 145–158 mA in the off status and 200–212 mA in the on status. After calculation based on the deviation of the above benchmark value, the feature interval  $\beta_1$  can be set to (-7, 6 mA), and the feature interval  $\beta_2$  can be set to (-6, 6 mA) to meet the recognition rate requirements under the normal status. The same analysis is carried out on voltage and power in the subsequent research, and the benchmark values and feature intervals of current, voltage, and power of this model of monitor are obtained in Table 5.

According to Table 3, the weight of voltage is set to 0 because of the overlap. The feature intervals for current and power have no overlap, and the weights can be set to 50% each. So far, the normal status benchmarks for the three main electrical characteristic parameters of a particular model of the monitor have been developed. There is no need to set further weight values as all characteristic cases are already covered.

**4.2. Measurement for Fault Event.** Next, this study is to investigate the fault statuses of this model of a monitor to check its features of fault. Through various experiments, it is found that air pump faults are more confusing when identified by a single parameter. Therefore, the fault analysis is carried out using an air pump fault as an example. Figure 11 is obtained by taking its current in the on and off statuses.

The overlap rate between the measured current value of the air pump fault and the normal feature interval is 70.2%, and the recognition rate is 29.8%, so the current can no longer meet the requirements of fault recognition, and it belongs to the special case of  $P'_1$  or  $P'_2$  in Figure 8, at which

point the other two features need to be collected and analyzed. The graphical comparison between the two types of electrical characteristic data and the normal threshold is shown in Figure 12.

From the above graph, it can be seen that the voltage cannot be distinguished in normal equipment, i.e., the recognition rate of the voltage is 0. The recognition rate of power is lower than 30% in the off status, but the recognition rate reaches 98.4% in the on status. According to Table 3, the weight values can be set as Table 6.

Bring the abovementioned air pump fault equipment back into working order. Collect the current of the normal equipment and compare it with the feature interval under the normal status, and the following comparison graph can be obtained in Figure 13.

The overall recognition rate for the normal status current is calculated to be 94.4%, and the thresholds set in Table 4 are proven to be feasible when the recognition rate for a single parameter reaches over 90%. The normal status of this model of a monitor can be accurately identified using the feature intervals in Table 5.

Next, additional test samples are added to further validate the air pump fault. The characteristic thresholds are optimized while validating the characteristic thresholds. Fifty monitors of the same model are subsequently selected for testing in this research. After sample control and data collection and analysis of the 10 units, their weights are then fine-tuned, and the final results of the characteristic values of the air pump fault obtained are shown in Table 7.

Besides the air pump fault, this paper aimed on the monitors to measure the following states:

- (1) ECG circuit module fault.
- (2) Motherboard fault.
- (3) Screen malfunction.
- (4) Main cable malfunction.

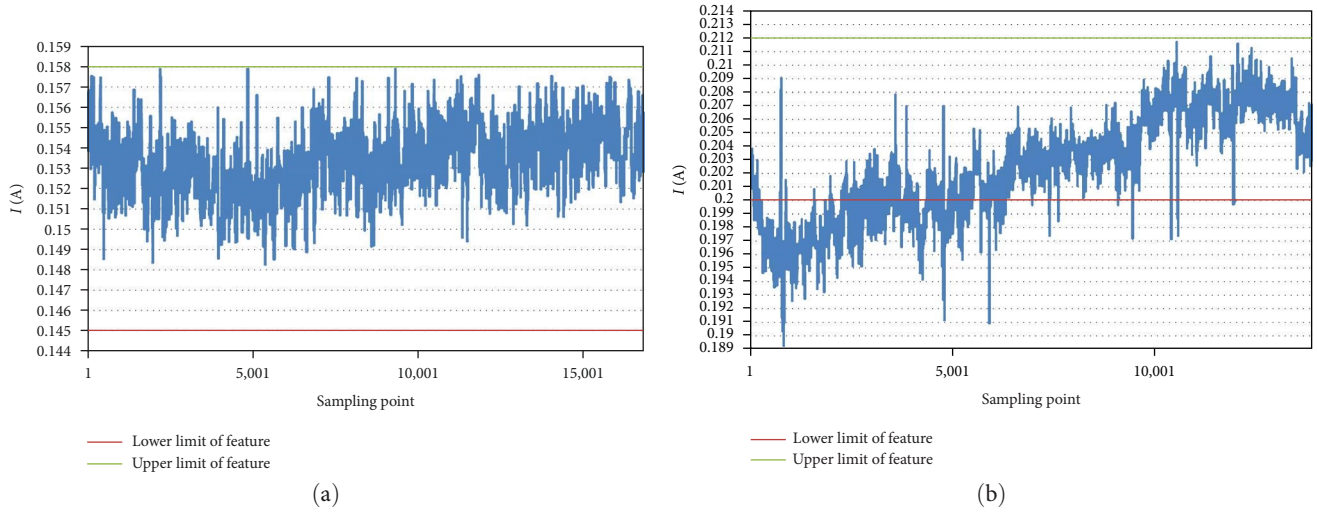


FIGURE 11: Comparison of air pump fault acquisition values with normal equipment characteristic intervals (a) off status (b) standby status.

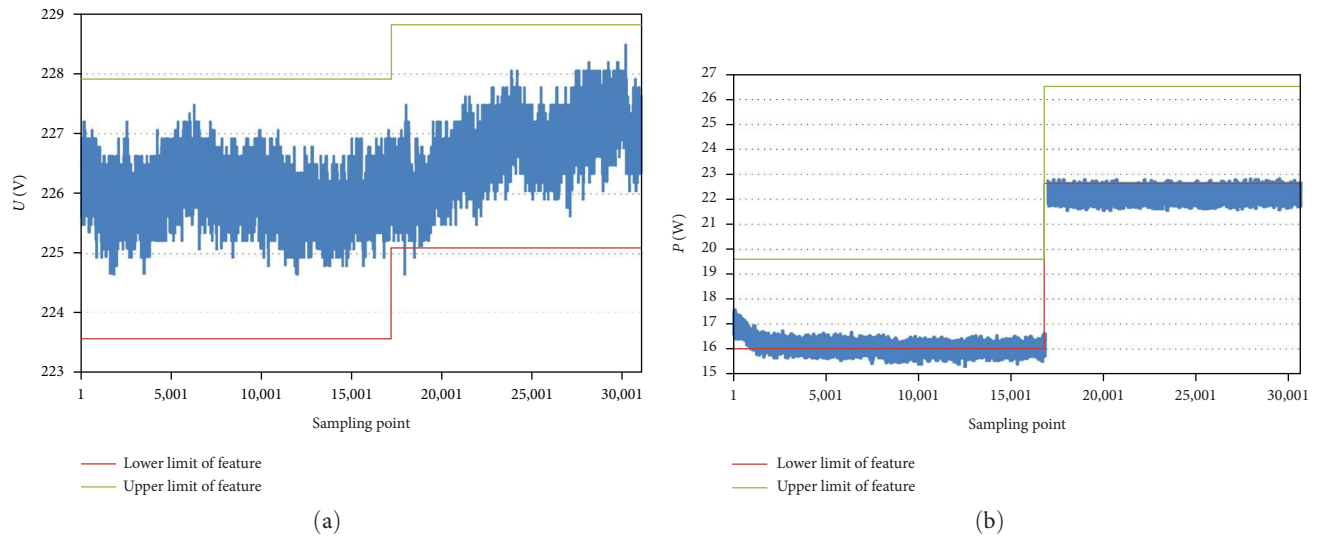


FIGURE 12: Voltage and power recognition graph of air pump faulty equipment (a) voltage (b) power.

TABLE 6: Corresponding weight of electrical features at each operation stage in case of air pump fault.

| Status | <i>I</i> |          |  | <i>V</i> |          |              | <i>P</i> |  |
|--------|----------|----------|--|----------|----------|--------------|----------|--|
|        | <i>P</i> | $\theta$ |  | <i>P</i> | $\theta$ | <i>P</i> (%) | $\theta$ |  |
| Off    | 0        | 0        |  | 0        | 0        | 45.2         | 4        |  |
| On     | 29.8%    | 2        |  | 0        | 0        | 98.4         | 9        |  |

Through a survey of medical engineer technicians, these fault states listed are common faults that occur on monitors. In order to understand these faults more clearly, this study collected these fault states and obtained the following data in Figure 14.

From the above data, it shows that each fault state can be well distinguished from the normal interval. There will not show the voltage and power data because we can set the

weight of the current in the on-off state of each fault to 100% so as to reach the 100% recognition rate of each fault except the main cable malfunction under off the power. It can be seen the normal interval overlaps with fault data a little bit. After calculating the rate of overlapping, it is only 3.6%. So we can also set the weight of the current in the on-off state of each fault to 100% to reach the following recognition:

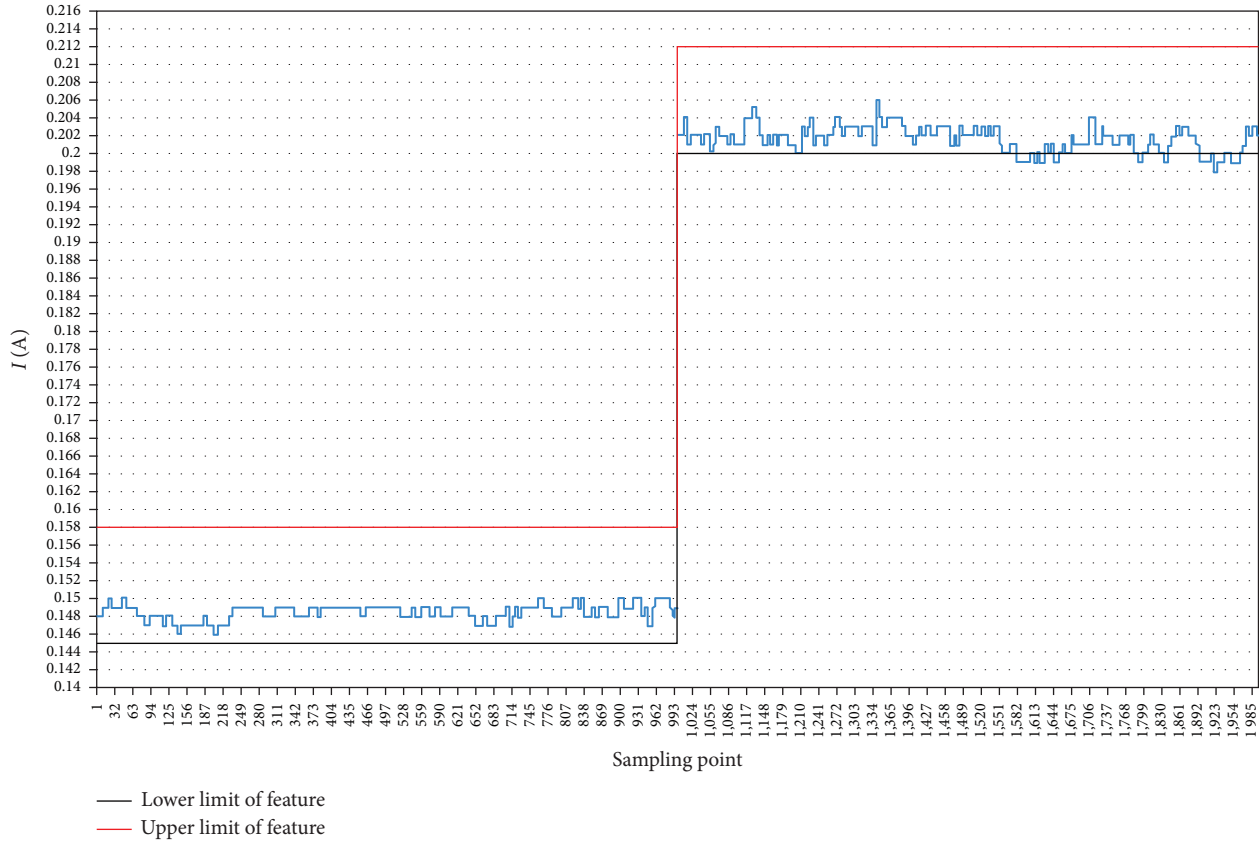


FIGURE 13: Comparison of the current of a normal equipment of the same model and feature interval under the normal status.

TABLE 7: Judgment rules for air pump fault of tenth monitors of the same model.

| Status and parameters | Current (mA) | Current weight (%) | Voltage (V)  | Voltage weight (%) | Power (W)    | Power weight (%) |
|-----------------------|--------------|--------------------|--------------|--------------------|--------------|------------------|
| Off                   |              |                    |              |                    |              |                  |
| Ave                   | 132          |                    | 224.25       |                    | 16.159       | 1.1              |
| $\beta, \chi, \delta$ | (-2,2)       | 0                  | (-0.62,0.35) | 0                  | (-0.11,0.08) |                  |
| Standby               |              |                    |              |                    |              |                  |
| Ave                   | 0.193        |                    | 225.94       |                    | 19.179       | 94.6             |
| $\beta, \chi, \delta$ | (-7,7)       | 4.3                | (-1.4,1.1)   | 0                  | (-0.55,0.43) |                  |

$$P = \frac{0 \times 4 + 96.4\% \times 1 + 100\% \times 99}{0 \times 4 + 1 + 99} = 99.96\%. \quad (13)$$

The molecule of Equation (13) represents six parameters: voltage, power, and current of on and off state. The recognition rate here can be infinitely close to 100% by adjusting the weight of current from on and off state.

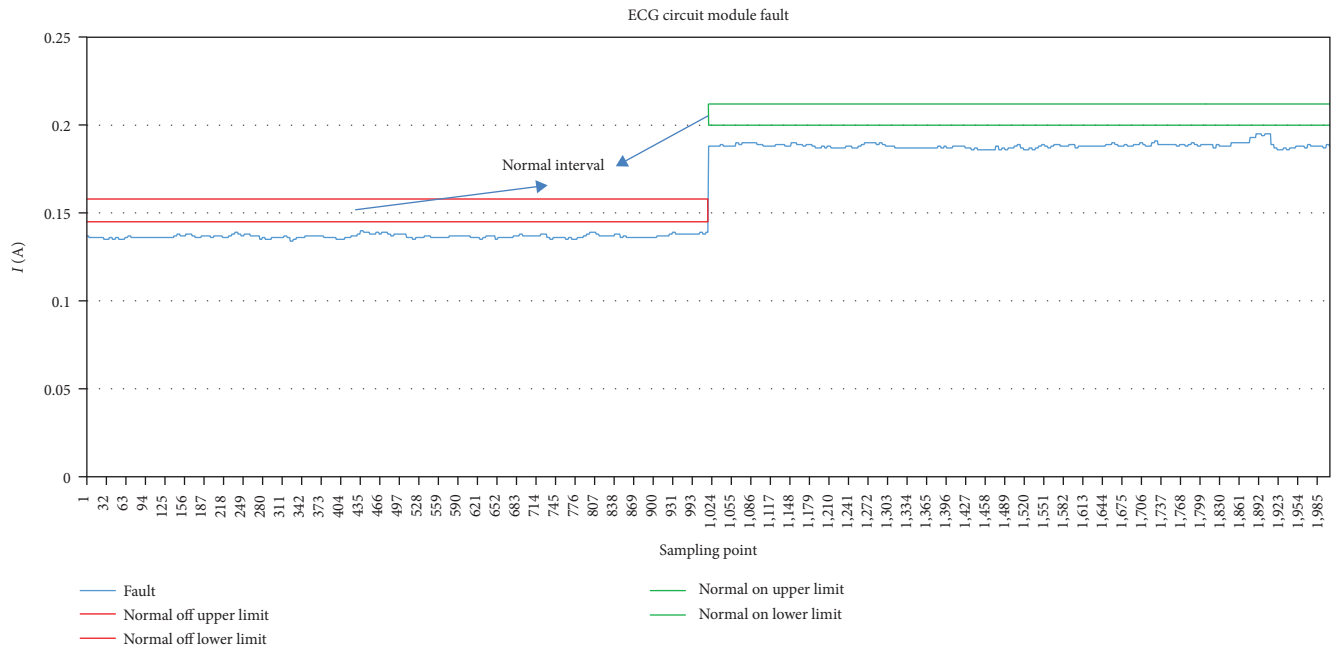
### 5. Discussion

The feature interval in the normal one of on and off status can be adjusted to achieve a 90% recognition rate within the minimum interval. But a 90% recognition rate is not the best result every time. So, combining the above data and adjusting the feature intervals several times in units of 1 mA, the following chart representing the relationship between the total

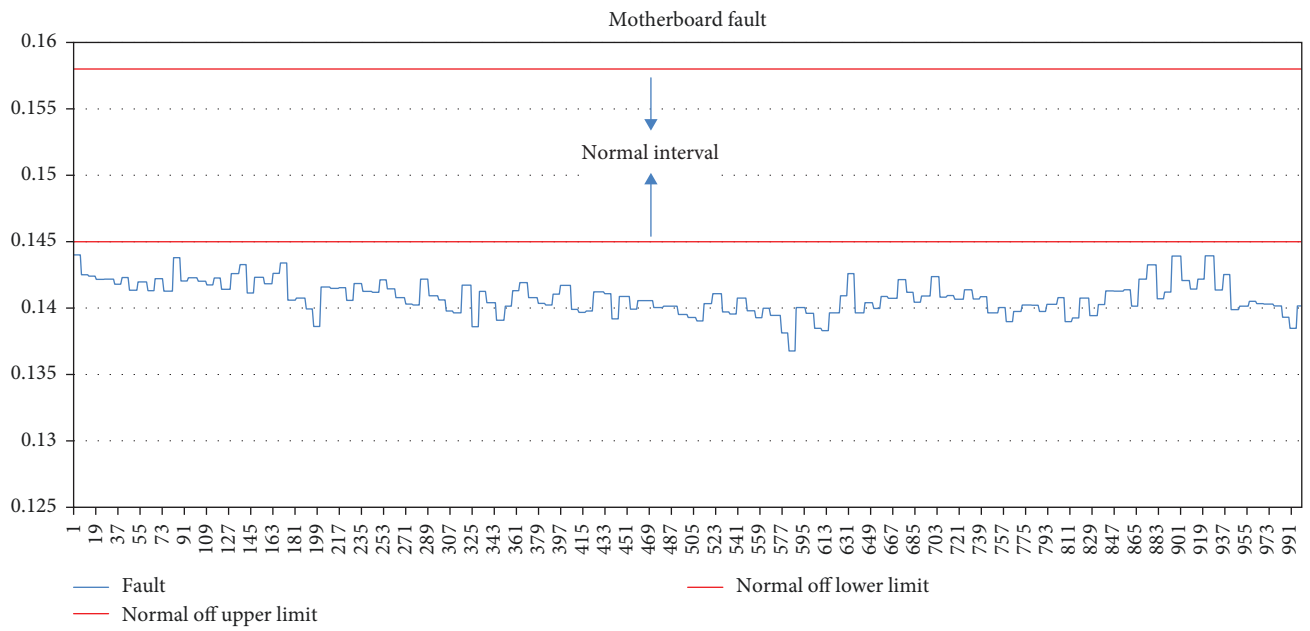
recognition rate and each characteristic interval can be obtained in Figure 15.

According to the characteristic values in Table 8, this paper found another 10 monitors with air pump faults that they are measured once again. It is found that the air pump fault recognition rate of 41 monitors could reach 90%. As the sample size increases, the weighting values can also be further fine-tuned in order to make the fault feature intervals more accurate. Although there are still 9 monitors with less than 90% of air pump faults identified using this feature in this research, in terms of 50 samples, the reliability of this method can reach more than 80%, which proves that this method is still worth promoting.

Using the above method, other faults of the monitor are analyzed. Due to a large number of fault types and the small sample space available for testing, weights are set according to the “0–1” rule, i.e., parameters with obvious features are

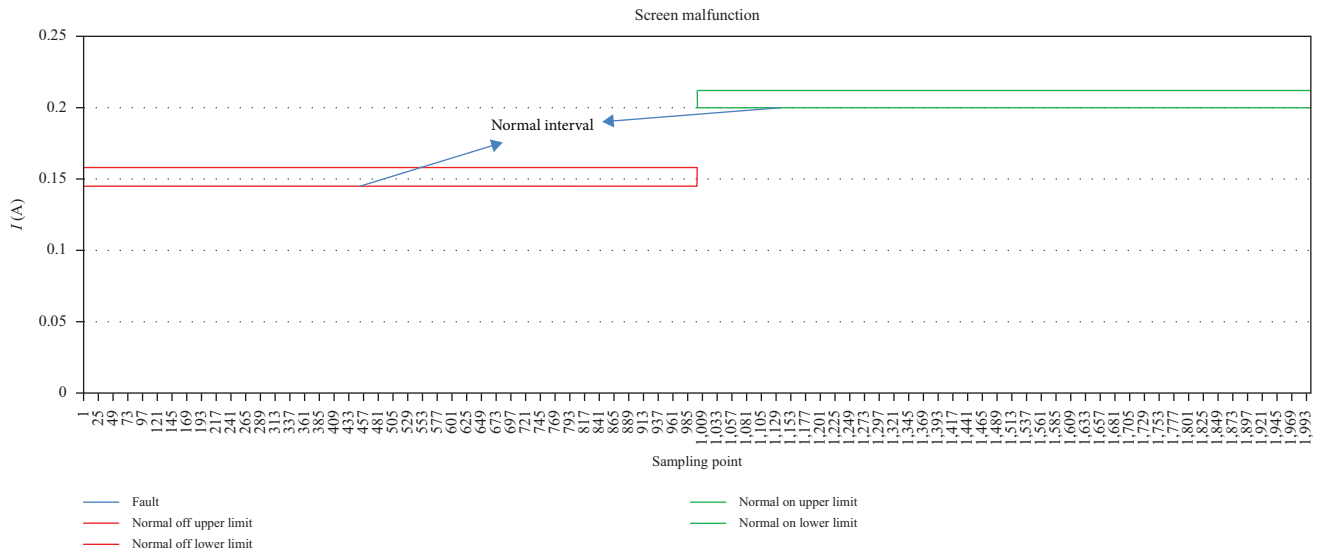


(a)

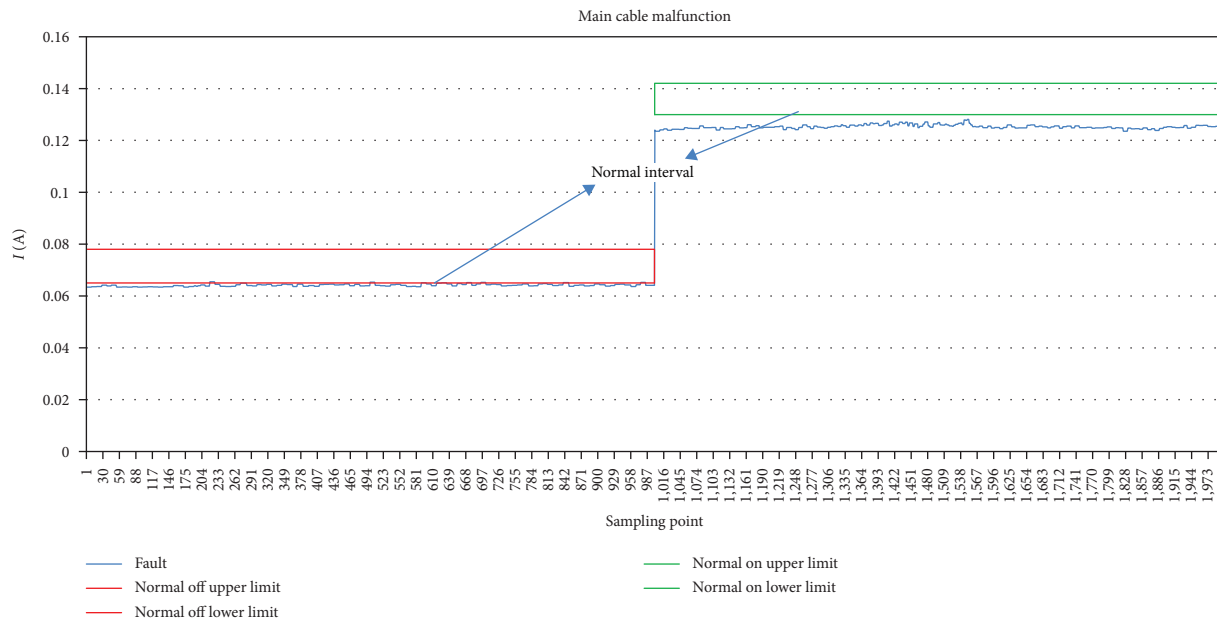


(b)

FIGURE 14: Continued.



(c)



(d)

FIGURE 14: (a) current of ECG circuit module fault and normal interval; (b) current of motherboard fault and normal interval; (c) current of screen malfunction and normal interval; (d) current of main cable malfunction and normal interval.

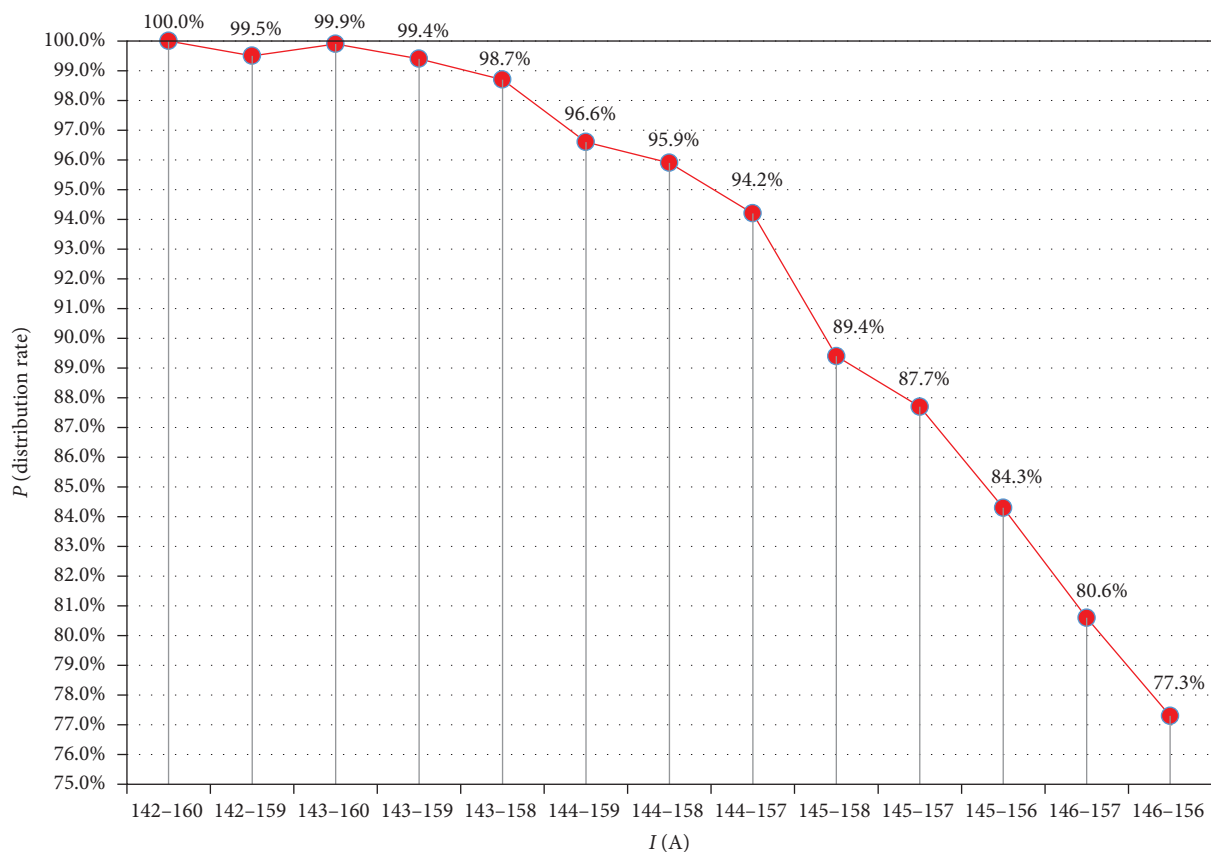
set to 100% weight, and the rest are set to 0. After statistical analysis, the following data are obtained.

Based on statistical data, it is now clear that the fault rule analysis method has a certain degree of validity. Through the collection and analysis of a large number of monitors' experimental data, it is concluded that multi-indicators can

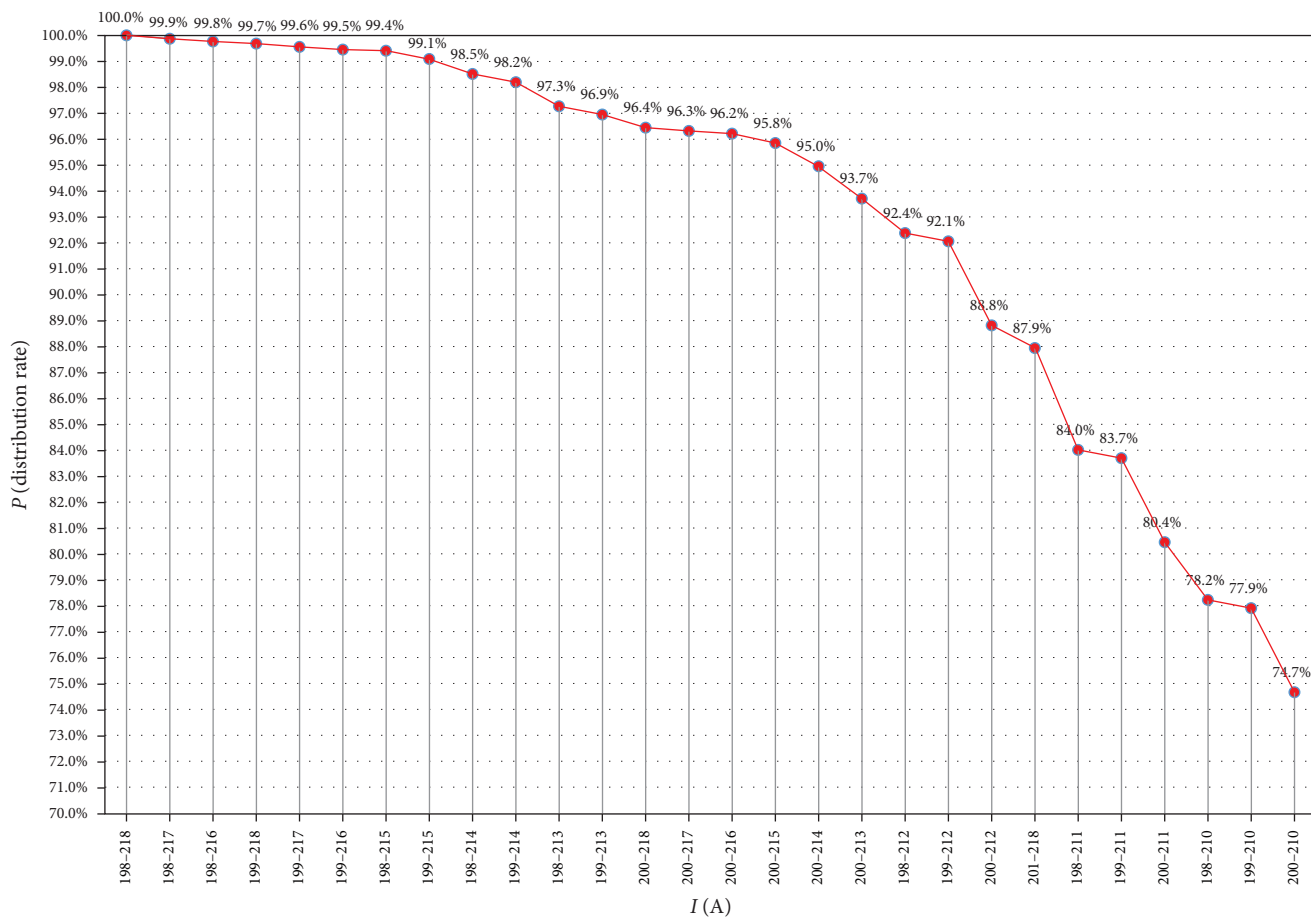
significantly improve the accuracy of fault detection, and the higher the accuracy of a parameter in a single indicator, the higher the accuracy rate of fault recognition under the fusion of multi-indicators.

For example, the air pump fault. From above, the recognition rate of air pump fault is the following:

$$P = \frac{0 \times 0 + 2 \times 29.8\% + 0 \times 0 + 0 \times 0 + 45.2\% \times 4 + 98.4\% \times 9}{0 + 2 + 0 + 0 + 4 + 9} = 75.1\%. \tag{14}$$



(a)



(b)

FIGURE 15: Relationship of total recognition rate versus each characteristic interval in the on and off statuses.

TABLE 8: Judgment accuracy rate of various indicators under different operating statuses.

| Statuses         | Normal (%) | ECG circuit module fault (%) | Motherboard fault (%) | Screen malfunction (%) | Main cable malfunction (%) | Air pump fault (%) |
|------------------|------------|------------------------------|-----------------------|------------------------|----------------------------|--------------------|
| Current only     | 100        | 48.1                         | 100                   | 85.3                   | 74.2                       | 30.5               |
| Voltage only     | 100        | 95.3                         | 89.2                  | 38.2                   | 26.5                       | 5                  |
| Power only       | 100        | 83.7                         | 80.1                  | 62.9                   | 81.5                       | 44.7               |
| Multi-indicators | 100        | 99.56                        | 100                   | 96.47                  | 97.3                       | 93.55              |

TABLE 9: Rules and conditions of air pump fault.

| Status and parameters | $I$ (mA) | $\theta_1$ (%) | $P$ (W)      | $\theta_2$ (%) | $U$ (V)      | $\theta_3$ (%) |
|-----------------------|----------|----------------|--------------|----------------|--------------|----------------|
| Off                   |          |                |              |                |              |                |
| Ave                   | 132      | 0              | 16.159       | 6.7            | 224.25       | 0              |
| $\beta, \chi, \delta$ | (-2,2)   |                | (-0.11,0.08) |                | (-0.62,0.35) |                |
| On                    |          |                |              |                |              |                |
| Ave                   | 0.193    | 3.3            | 19.179       | 90             | 225.94       | 0              |
| $\beta, \chi, \delta$ | (-7,7)   |                | (-0.55,0.43) |                | (-1.4,1.1)   |                |

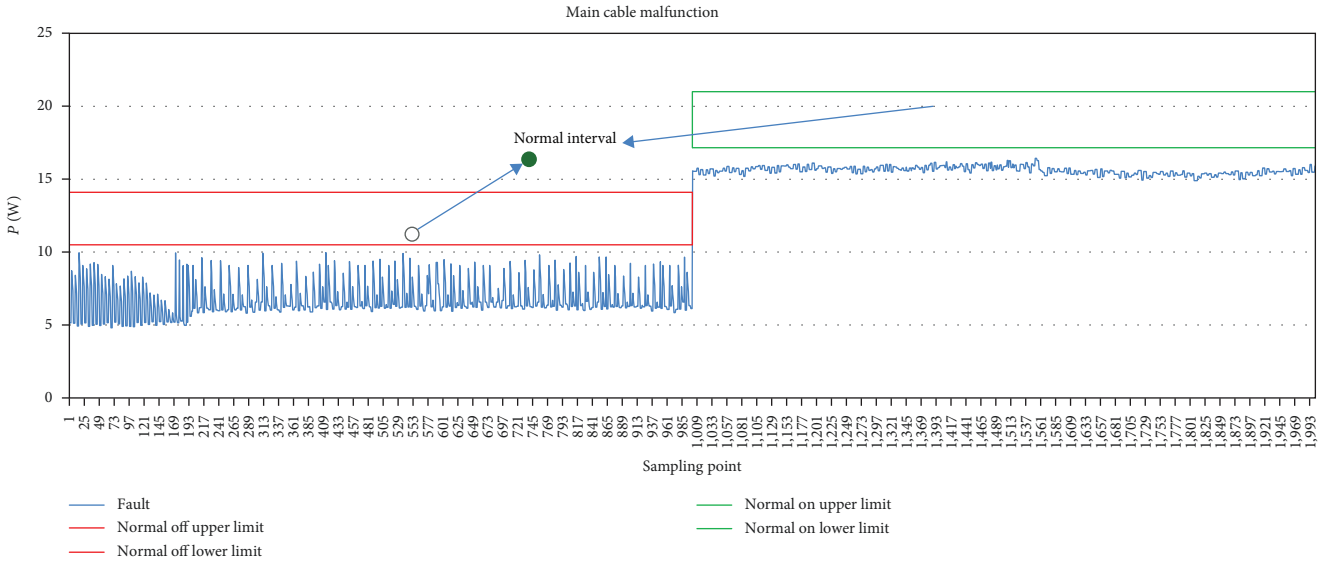


FIGURE 16: The power of main cable malfunction and normal interval.

At present, the total recognition rate of air pump faults is only 75.1%. After adjusting the key weight, the overall recognition rate of air pump fault reaches 92.7% while the final weight setting is  $\theta_1 = [0, 0.5], \theta_2 = [0, 0], \theta_3 = [1, 13.5]$ . It is in the line with the research objective of this paper. The judgment rules of the air pump fault under the current hardware conditions are set in Table 9.

If the actual situation is that it is necessary to reach 100% of the recognition rate, taking the main cable malfunction in Figure 14 as an example, we can introduce another two electrical performance parameters. After measurement and analysis, the power during the main cable malfunction can be expressed, as shown in Figure 16.

The result shows that there is no overlap between the normal power interval and the main cable malfunction data, so the recognition rate can reach 100%. Therefore, we can set the following weights to achieve a 100% recognition rate:

$$P = \frac{0 \times 2 + 100 \times 1 + 100 \times 1 + 96.4\% \times 0 + 100\% \times 1}{0 \times 3 + 1 + 1 + 1} = 100\% \tag{15}$$

This is the advantage of introducing MEPP for joint recognition of fault events: the expected recognition rate can be achieved by constantly adjusting the weight of the features.

However, here comes a problem with these threshold values: some intervals of electrical features seem to be overlap with others' intervals. It will cause the recognition fuzzy. Through adding test samples, the result shows that overlapping parts would not affect the recognition. The interval is shown in Figure 17.

It indicates that the overlapping interval has a great influence on the recognition rate. After statistical calculation, this



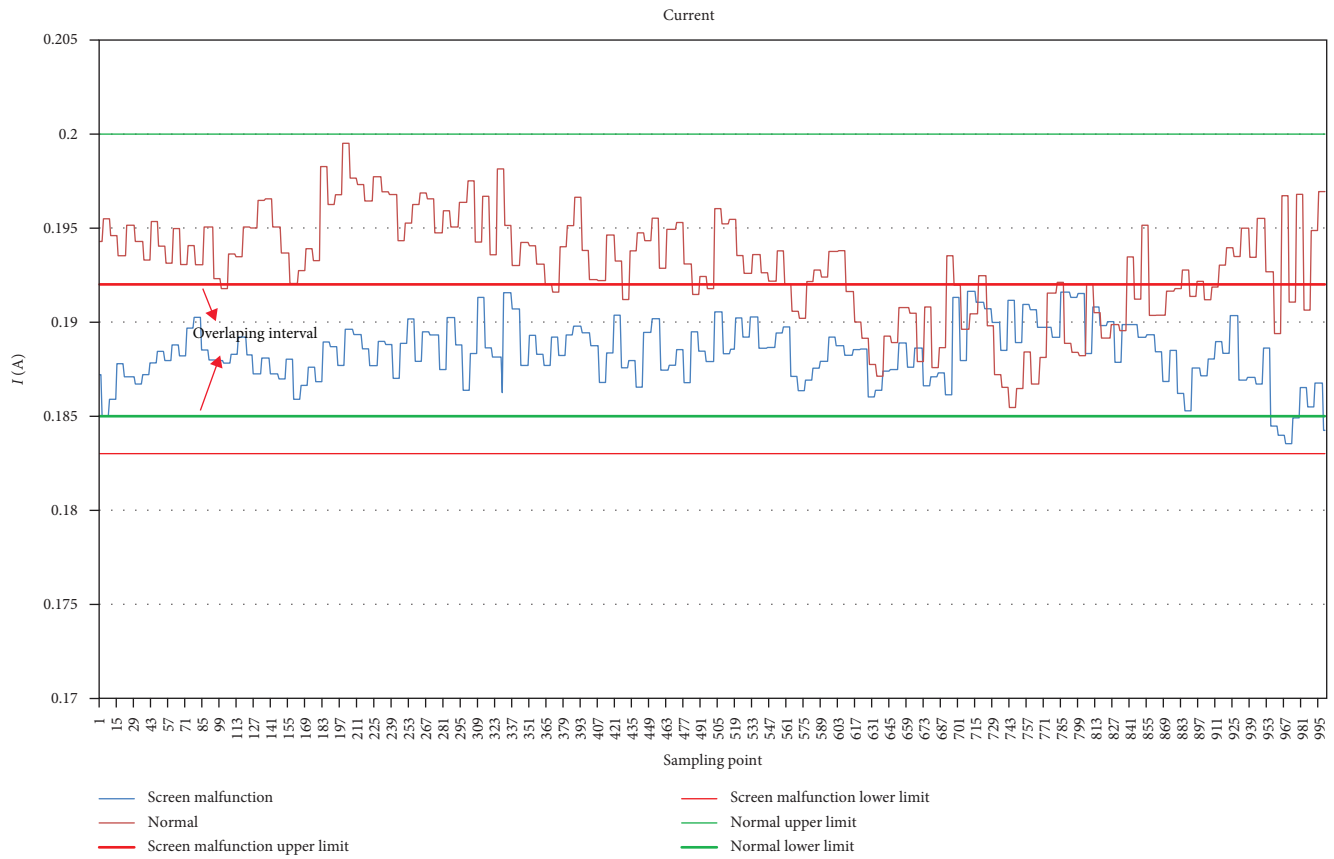


FIGURE 17: The monitors' current of screen malfunction and normal.

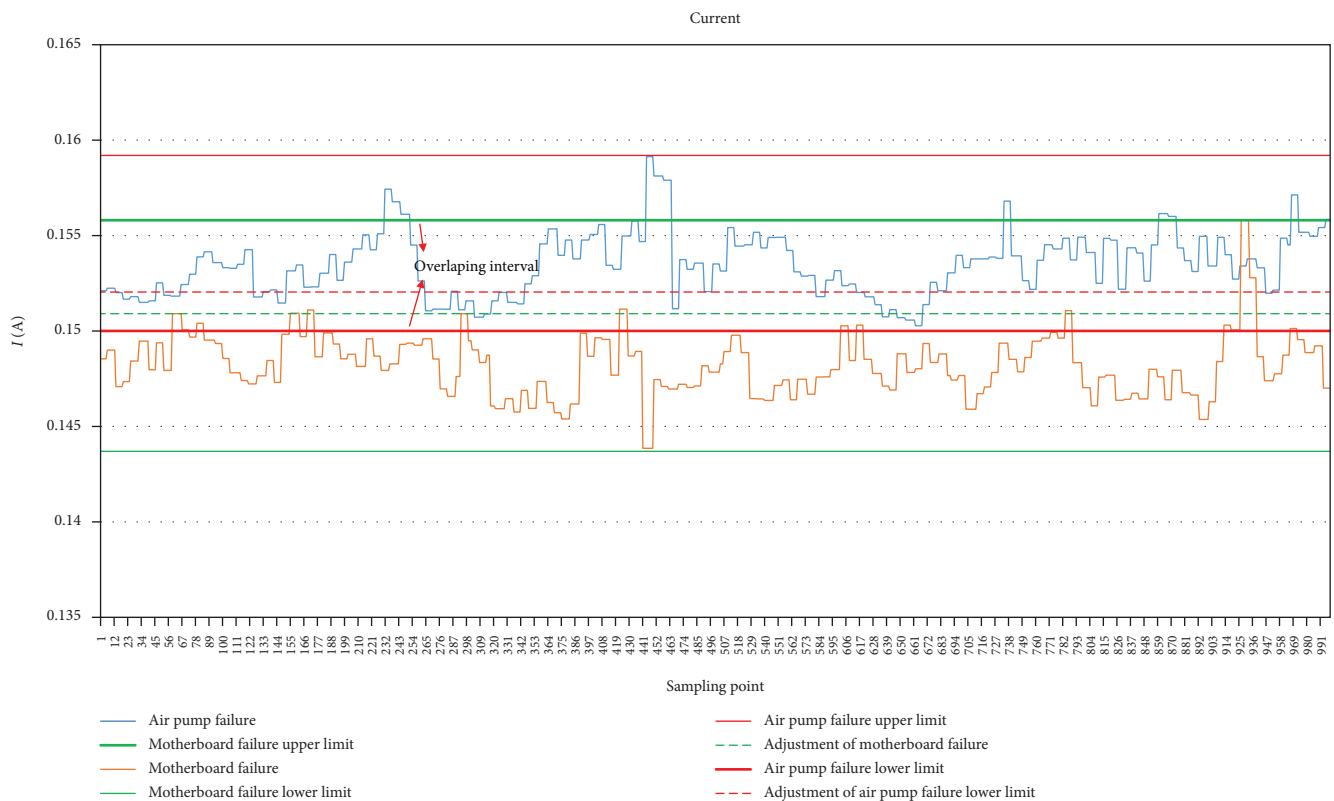


FIGURE 18: Fault rules of the monitor screen malfunction with normal current before adjustment.

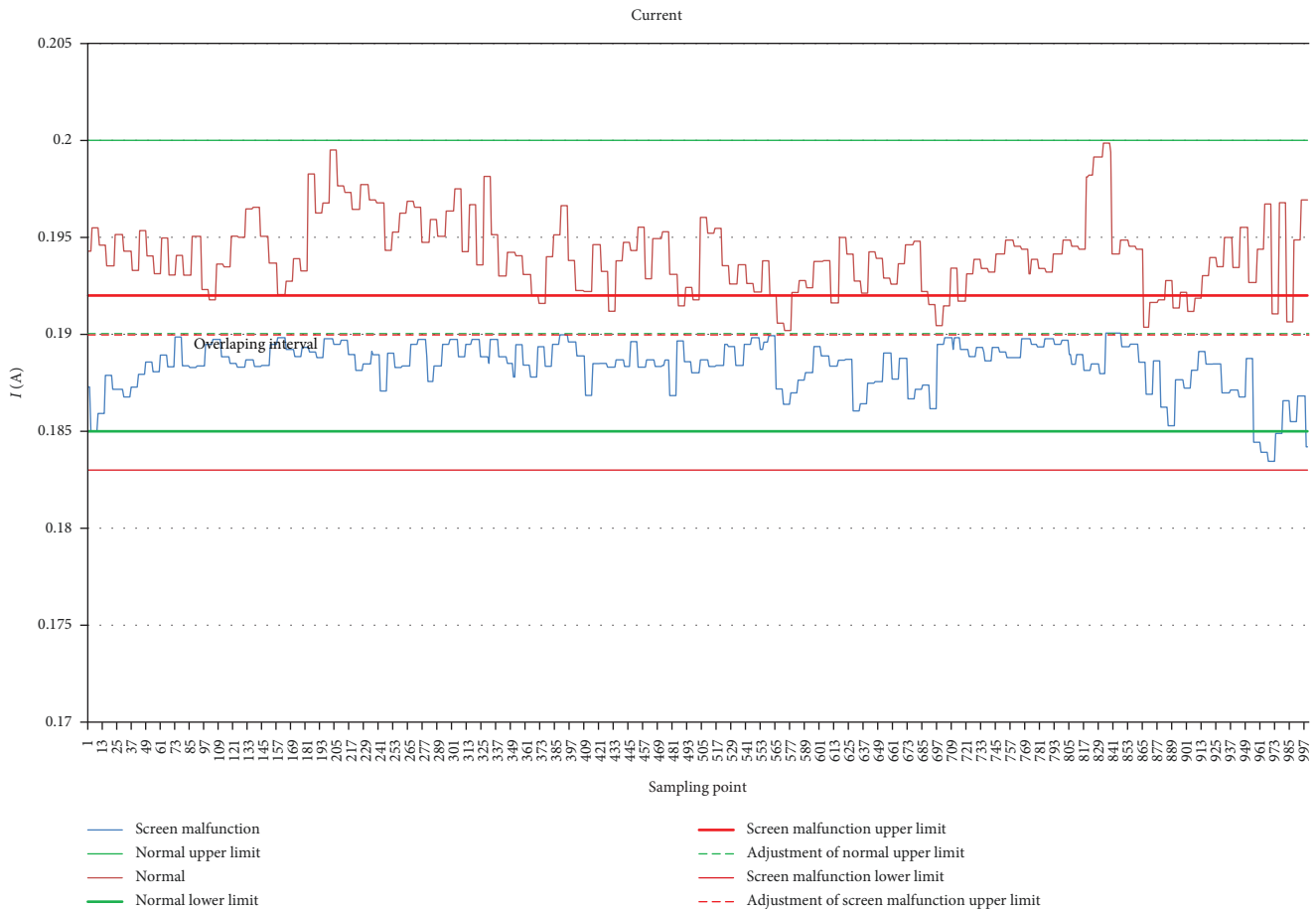


FIGURE 19: Fault rules of the monitor screen malfunction with normal current after adjustment.

paper will use the difference compensation method to adjust the threshold. Specific steps are as follows:

- (1) Take the characteristic interval of a normal state as the reference interval.
- (2) Take out the sample points in the overlapping part from the measured data.
- (3) Calculate the recognition rate of different intervals in the new state.
- (4) Compare the recognition rate. In principle, the new interval of state should not overlap with the normal interval. The data proceed as shown in Figure 18.

After the adjustment, the recognition rate will follow the change law of Figure 15. Because this study can be applied to any electronic device, there is no standard recognition rate value that can be applied to all relevant fields. The accuracy rate should be set suitable for the specific situation. This paper will choose the 90% as a research basis.

Sometimes, we found even if we use this method, it cannot avoid the overlap unless needing to sacrifice a lot of recognition accuracy (like Figure 17). In this case, we can identify and compensate for obvious outliers by improving the Z-score method. The specific method is to determine the reference mean of the whole data of a single measurement

first. Then, it will recognize the outlier by the Z-score method. When the outlier is identified, the reference mean of this measurement is used to compensate the outlier, so as to make up for the range error caused by the outlier. Taking Figure 15 as an example, using the improved Z-score method for interval adjustment, as shown in Figure 19.

The dashed line is the adjusted interval. After optimization by the improved Z-score method, the interval of the two states is clearly distinguished. It is proven that the improved Z-score method is very suitable for data processing in the basic research of electrical performance features. After the adjustment, the recognition rate still keeps upon 90%.

## 6. Conclusion

The multi-indicator-based fault detection method used in this paper can not only overcome the difficult situation of logical confusion in multi-indicator judgment but also greatly increase the types of identifiable faults and improve the recognition rate of a single fault. This method successfully combines the theoretical model with the empirical facts and realizes the mathematical model, feature extraction, and system design of fault identification of various electrical performance parameters through the correlation between the characteristics of electrical performance parameters and fault

events. The innovation of this research lies mainly in its ability to address the following difficulties in medical equipment fault recognition research.

- (1) It has simplified the detection process. In line with the trend toward device fault detection, this research looks at medical equipment as a whole to do current fault detection. This method greatly simplifies the operation of the detection process, increases the operability of current fault detection, and has the potential to be widely popularized. Furthermore, contrary to the device-based fault recognition derivation logic, this method can compensate for the lack of theoretical research in fault recognition.
- (2) It has summarized prior knowledge into a mature fault database, which covers malfunction types, judgment methods, recognition rules, malfunction features, etc. This is the first time that the content of system-level medical equipment fault recognition has been summarized since the aerospace field, which can provide a reference for follow-up research.
- (3) This research has made up for the shortcomings of single feature factors in system-level fault recognition, greatly improving recognition accuracy and increasing the identifiable malfunction types.
- (4) This research has established a fault recognition system with a very high degree of openness. The system can be updated through continuous optimization, and the introduction of new knowledge, and the research direction will not be terminated because of certain technical obstacles.

However, the method still needs to be tested on a large number of experimental samples before it can be used to build a knowledge base. In addition, with the increase in the amount of data, traditional statistical methods have been unable to meet the needs of data processing, and machine learning methods need to be introduced to process massive sample data more quickly. With the further application of this method in the field of medical devices, this research direction will continue to explore more meaningful relevant results.

### Data Availability

The data used to support the findings of this study are available from the corresponding author upon request.

### Conflicts of Interest

The authors declare that they have no conflicts of interest.

### Acknowledgments

This study was funded by the Chongqing Science and Technology Bureau, 2022MSXM060, and the Chongqing Health Commission, cstc2019jscx-msxmX0183.

### References

- [1] J. Gai and Y. Hu, "Research on fault diagnosis based on singular value decomposition and fuzzy neural network," *Shock and Vibration*, vol. 2018, Article ID 8218657, 7 pages, 2018.
- [2] Y. Lei, B. Yang, X. Jiang, F. Jia, N. Li, and A. K. Nandi, "Applications of machine learning to machine fault diagnosis: a review and roadmap," *Mechanical Systems and Signal Processing*, vol. 138, Article ID 106587, 2020.
- [3] W. Song, X. Liu, J. Zhao, M. Wang, and Y. Liu, "Research on the intelligent identification method of the substation equipment faults based on deep learning," in *2020 IEEE International Conference on Power, Intelligent Computing and Systems (ICPICS)*, vol. 30, pp. 888–891, IEEE, Shenyang, China, July 2020.
- [4] J. Liu, Y. Chen, and H. Jiang, "Universal fault and diagnosis method of expert KB on regulation," *Computer & Digital Engineering*, vol. 38, no. 6, pp. 72–76, 2010.
- [5] P. Li, W. Di, and G. Xiong, "Research on fault detection of complex medical equipment based on association mining," *China Academic Journal Electronic Publishing House*, vol. 32, no. 12, pp. 48–56, 2017.
- [6] Z. Zhang and X. Zhang, "Fault diagnosis method of railway signal equipment based on association rules," *Railway Standard Design*, vol. 66, no. 4, pp. 175–181, 2022.
- [7] A. Yan, L. Yu, and P. N., "Fault diagnosis method by case-based reasoning for reverse osmosis membrane," *Journal of Beijing University of Technology*, vol. 44, no. 11, pp. 1396–1400, 2018.
- [8] H. Cui and F. Cheng, "Fault diagnosis of mine main ventilator based on improved fuzzy reasoning theory," *Coal Technology*, vol. 40, no. 10, pp. 112–115, 2021.
- [9] H. Chen, A. Zhao, T. Li, C. Cai, S. Cheng, and C. Xu, "Fuzzy Bayesian network inference fault diagnosis of complex equipment based on fault tree," *Systems Engineering and Electronics*, vol. 43, no. 5, pp. 1248–1261, 2021.
- [10] S. Zhang, L. Lang, and Y. Chong, "Research on fault diagnosis method of switching power supply based on feature fusion," *China Academic Journal Electronic Publishing House*, vol. 37, no. 9, pp. 27–32, 2022.
- [11] D. Neupane and J. Seok, "Bearing fault detection and diagnosis using case Western Reserve University dataset with deep learning approaches: a review," *IEEE Access*, vol. 8, pp. 93155–93178, 2020.
- [12] M. S. Lazeregue, H. Salhi, and M. Tadjine, "Analytical and neuro-fuzzy modeling for fault detection and identification for nonlinear systems: application to robot manipulator," *Archives of Control Sciences*, vol. 19, no. 3, pp. 325–350, 2009.
- [13] S. Zhang, Y. Chong, J. Xiao, P. Zhao, and X. Jin, "Medical equipment fault diagnosis system based on LabVIEW," *Instrument Technique and Sensor*, no. 4, pp. 98–103, 2018.
- [14] L. T. DeCarlo, "Signal detection theory and generalized linear models," *Psychological Methods*, vol. 3, no. 2, pp. 186–205, 1998.
- [15] X. Wen, D. Chen, and Y. Qiao, "Neural network fault diagnosis technology and its application on spacecraft in China," *Journal of Shenyang Aerospace University*, vol. 35, no. 3, pp. 17–26, 2018.
- [16] N. D. Sidiropoulos, L. De Lathauwer, X. Fu, K. Huang, E. E. Papalexakis, and C. Faloutsos, "Tensor decomposition for signal processing and machine learning," *IEEE Transactions on Signal Processing*, vol. 65, no. 13, pp. 3551–3582, 2017.

- [17] X. Yu, M. Wang, P. Zhang, and J. Lin, "Electrical Identification and monitoring based on single-phase electrical parameters," *New Product & Tech*, vol. 18, no. 7, pp. 65–67, 2018.
- [18] P. Lu, R. Zhang, G. Wu, and T. Hu, "A new security event correlation analysis engine based on rule-tree-matching," in *2022 IEEE 5th Advanced Information Management, Communicates, Electronic and Automation Control Conference (IMCEC)*, pp. 29–33, IEEE, Chongqing, China, December 2022.